

Catalysis of the Methanolysis of Activated Amides by Divalent and Trivalent Metal Ions. The Effect of Zn^{2+} , Co^{2+} , and La^{3+} on the Methanolysis of Acetylimidazole and Its $(\text{NH}_3)_5\text{Co}^{\text{III}}$ Complex

Alexei A. Neverov, Pedro J. Montoya-Pelaez, and R. S. Brown*

Contribution from the Department of Chemistry, Queen's University, Kingston, Ontario, K7L 3N6 Canada

Received July 3, 2000

Abstract: The metal ions Zn^{2+} , Co^{2+} , and La^{3+} strongly catalyze the methanolysis of the activated amides acetylimidazole (**1**) and its ligand-exchange-inert Co^{III} complex, $(\text{NH}_3)_5\text{Co}^{\text{III}}\text{-AcIm}$ (**2**). Studies of the kinetics of methanolysis are performed with pH measurement and control, and the metal ions are soluble in the medium throughout the pH regions where ionization of the $\text{M}^{x+}(\text{CH}_3\text{OH})_y$ occurs. Zn^{2+} and Co^{2+} act as Lewis acids toward **1**, catalyzing attack of external methoxide on a **1**: M^{2+} complex at values only 100-fold lower than the diffusion limit, the k_{OR} values being $5.6 \times 10^7 \text{ M}^{-1} \text{ s}^{-1}$ and $2.5 \times 10^7 \text{ M}^{-1} \text{ s}^{-1}$, while that for CH_3O^- attack on **2** is $4.69 \times 10^7 \text{ M}^{-1} \text{ s}^{-1}$. Since neither Zn^{2+} nor Co^{2+} promotes the methanolysis of **2**, these metals appear to be acting through transient binding to the distal N of **1**, which activates the $\text{C}=\text{O}$ of the complex to external CH_3O^- attack. La^{3+} catalyzes the methanolysis of both **1** and **2**, which occurs by a mechanism that is fundamentally different from that exhibited by Zn^{2+} and Co^{2+} in that the active species appears to be a bis-methoxy-bridged dimer $(\text{La}^{3+})_2(\text{CH}_3\text{O}^-)_2(\text{CH}_3\text{OH})_x$ that interacts directly with the $\text{C}=\text{O}$ unit of the substrate.

Introduction

Metal ion catalysis of the hydrolysis¹ of esters and amides in aqueous solution has been well studied due to the biological implications of these and the fact that many Zn^{2+} -containing enzymes promoting these reactions are known.² One of the major stumbling blocks in understanding metal ion catalysis of hydrolyses is the fact that, above the pK_a 's of the metal–aquo species, formation of metal hydroxide precipitates and gels often complicates mechanistic analysis.³ The problem of precipitation

above the $\text{M}^{x+}(\text{H}_2\text{O})_y \text{pK}_a$ has, in many cases,¹ been circumvented through binding of the metal ions to complexing ligands, but even so it is usually difficult to study the reactions under highly basic conditions.

We have embarked on an extensive investigation of metal ion catalysis of methanolysis of carbon and phosphorus esters and amides. Among organic solvents, methanol is the closest to water in structure and properties, so in some ways methanolysis reactions are anticipated to resemble hydrolysis reactions. However, there can be important differences, particularly for metal-ion-promoted reactions, attributable to a reduced dielectric constant relative to water (31.5 vs 78.5 at 25 °C)⁴ that might be relevant to the local dielectric constant of the enzyme interior.⁵ Nevertheless, methanolysis reactions have not been studied nearly so extensively as hydrolysis reactions, probably due to difficulties in determining and controlling pH in methanol. Recent reports by Bosch and co-workers⁶ have shown that the pH in methanol (pH) can be measured simply by using a glass electrode, and they have presented an extensive list^{6b} of pK_a values for species that would be useful as buffering agents in methanol. While originally investigated for applications in HPLC separations, these contributions suggest that it should now be possible to run detailed pH vs rate studies for a variety of important processes in buffered methanol as easily as in water. To our knowledge, this does not appear to have been attempted even for simple systems.

(1) Przystas, T. J.; Fife, T. H. *J. Chem. Soc., Perkin Trans. 2* **1990**, 393 and references therein. (b) Suh, J. *Acc. Chem. Res.* **1992**, 25, 273 and references therein. (c) Tecilla, P.; Tonellato, U.; Veronese, F.; Fellugg, F.; Scrimin, P. *J. Org. Chem.* **1997**, 62, 7621. (d) Chin, J.; Jubian, V.; Mrejen, K. *J. Chem. Soc., Chem. Commun.* **1990**, 1326. (e) Meriwether, L.; Westheimer, F. *J. Am. Chem. Soc.* **1956**, 78, 5119. (f) Grant, T. J.; Hay, R. W. *Aust. J. Chem.* **1965**, 18, 1189. (g) Groves, J. T.; Dias, R. M. *J. Am. Chem. Soc.* **1979**, 101, 1033. (h) Groves, J. T.; Chambers, R. R. *J. Am. Chem. Soc.* **1984**, 106, 630. (i) Groves, J. T.; Olson, J. R. *Inorg. Chem.* **1985**, 24, 2715. (j) Sayre, L.; Reddy, K. V.; Jacobson, A. R.; Tang, W. *Inorg. Chem.* **1992**, 31, 935. (k) Fife, T. H. *Acc. Chem. Res.* **1993**, 26, 325. (l) Fife, T. H.; Bembi, R. *J. Am. Chem. Soc.* **1993**, 115, 11358. (m) Parac, T. N.; Kostić, N. M. *J. Am. Chem. Soc.* **1996**, 118, 51. (n) Singh, L.; Ram, R. N. *J. Org. Chem.* **1994**, 59, 710. (o) Sutton, P. A.; Buckingham, D. A. *Acc. Chem. Res.* **1987**, 20, 357. (p) Kimura, E.; Nakamura, I.; Koike, T.; Shionoya, M.; Kodama, Y.; Ikeda, T.; Shiro, M. *J. Am. Chem. Soc.* **1994**, 116, 4764. (q) Parac, T. N.; Ullman, G. M.; Kostić, N. M. *J. Am. Chem. Soc.* **1999**, 121, 3127 and references therein. (r) Ridder, A. M.; Kellogg, R. M. In *Supramolecular Reactivity and Transport: Bioorganic Systems*; Comprehensive Supramolecular Chemistry Vol. 4; Murakami, Y., Ed.; Elsevier Science Ltd.: Oxford, 1996; Chapter 11. (s) Chin, J. *Acc. Chem. Res.* **1991**, 24, 145 and references therein.

(2) Lipscomb, W.; Sträter, N. *Chem. Rev.* **1996**, 96, 2375. (b) Coleman, J. E. *Curr. Opin. Chem. Biol.* **1998**, 2, 222.

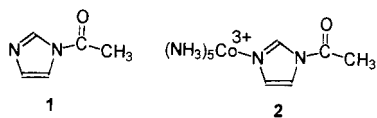
(3) Rustad, J. R.; Dixon, D. A.; Rosso, K. M.; Felmy, A. R. *J. Am. Chem. Soc.* **1999**, 121, 324. (b) Baes, C. F.; Mesmer, R. E. *Hydrolysis of Cations*; R. E. Krieger Publishing Co.: Malabar, FL, 1976. (c) Smith, R. M.; Martell, A. E. *Inorganic Complexes; Critical Stability Constants Vol. 4*; Plenum Press: New York, 1976. (d) Richens, D. T. *The Chemistry of Aquo Ions*; John Wiley and Sons: New York, 1997.

(4) Harned, H. S.; Owen, B. B. *The Physical Chemistry of Electrolytic Solutions*, 3rd ed.; ACS Monograph Series 137; Reinhold Publishing: New York, 1957; p 161.

(5) Ferscht, A. *Enzyme Structure and Function*, 2nd ed.; W. H. Freeman and Co.: New York, 1985; pp 64–69.

(6) Bosch, E.; Rived, F.; Roses, M.; Sales, J. *J. Chem. Soc., Perkin Trans. 2*, **1999**, 1953. (b) Rived, F.; Rosés, M.; Bosch, E. *Anal. Chim. Acta* **1998**, 374, 309. (c) Bosch, E.; Bou, P.; Allemann, H.; Roses, M. *Anal. Chem.* **1996**, 3651.

In the following we report a detailed kinetic investigation of the methanolysis of the activated amide, acetylimidazole (**1**),⁷ and its ligand-exchange-inert Co³⁺ complex, *N*-acetylimidazole-pentaaminecobalt(III), (AcImCo(NH₃)₅)³⁺, (**2**).⁸ These substrates



were chosen in part because the mechanisms of their hydrolyses are well understood,^{7,8} which allows ready comparison with their methanolyses, and in part because, despite extensive study, it has yet to be shown that **1** undergoes significant metal-ion-promoted acceleration of its hydrolysis. Fife and co-workers have shown^{1a,k,l} that *N*-acylimidazoles and *N*-acylbenzimidazoles that incorporate proximal metal-binding sites do undergo M²⁺-catalyzed hydrolyses, but in the absence of such binding sites, or when metal binding occurs away from the scissile (N)C=O unit, catalysis is not observed. Indeed, such binding appears to be a general requirement for strong metal ion catalysis of the hydrolysis of more normal amides as well,^{1f-j,m-q} since those without proximal binding sites typically do not exhibit metal ion catalysis of hydrolysis. As will be shown, strong metal ion catalysis of the methanolyses of **1** and **2** by Zn²⁺, Co²⁺, and La³⁺ is observed, so that a proximal metal-binding site appears unnecessary in MeOH solution although amides containing such may well be even more susceptible to metal-ion-promoted methanolysis. Furthermore, our studies show that, in MeOH, the La³⁺ and Zn²⁺ metal ions remain in solution throughout the entire pH domain where M⁺(MeOH)_y ionizes to form metal-bound methoxides, thus avoiding the problems of insoluble metal-containing precipitates inherent in analogous studies in water.

Experimental Section

Materials. *N*-Acetylimidazolepentaaminecobalt(III) perchlorate, [(NH₃)₅CoImCOCH₃](ClO₄)₃ (**2**), was prepared as previously described.⁸ Methanol (99.8% anhydrous), sodium methoxide (0.5 M), HClO₄ (70%, BDH), acetonitrile (99.8% anhydrous), acetylimidazole, Zn(ClO₄)₂·6H₂O, Co(ClO₄)₂·6H₂O, and La(CF₃SO₃)₃ were all purchased from Aldrich and used without any further purification.

pH Measurements. The CH₃OH₂⁺ concentration was determined by using a Radiometer GK2322 combination (glass/calomel) electrode calibrated with Fisher Certified standard aqueous buffers (pH = 4.00 and 10.00). Values of ^spH were calculated by adding the correction constant (2.24) to the experimental meter reading (^wpH). This method was first described by Bates⁹ for a molality scale (correction constant 2.34), and later by Bosch et al.⁶ for a molar correction constant. The ^spK_a's of buffers used for the present kinetic studies were measured at half-neutralization of the bases with 70% HClO₄ in MeOH.

^spK_a Determination. The potentiometric titrations of the above metal salts in methanol were performed using a Radiometer Vit 90 autotitrator under anaerobic conditions (Ar) at ambient temperature. The concentrations of metal salts and sodium methoxide titrant

(prepared from stock 0.5 M methoxide provided in a Sure Seal bottle) were (1.00–1.33) × 10⁻³ and (1.88–2.00) × 10⁻³ M, respectively. The latter was calibrated by titrating standardized HCl with the endpoint taken to be ^spH = 8.38. The values of the dissociation constants (^spK_a) were calculated by using the computer program PKAS.¹⁰ The ^wpK_w in the program was replaced by the autoprotolysis constant for methanol at 25 °C (^spK_{MeOH} = 16.77).⁶ In the cases of Zn²⁺ and Co²⁺, the titration data were treated according to eq 3 (below), and values of K_{app} (the product of the two dissociation constants for sequential removal of CH₃O⁻ from M²⁺(CH₃O⁻)₂) were calculated by an NLLSQ fit of the experimental data to the following equation:

$${}^s\text{pH} = {}^s\text{p}K_{\text{MeOH}} - {}^s\text{p}K_{\text{app}}/2 + 0.5 \log(V_{\text{base}}C_{\text{base}}/(2V_{\text{init}}[\text{M}^{2+}]_{\text{total}} - V_{\text{base}}C_{\text{base}}))$$

where *V* represents volume and *C* concentration. ^sK_a values were calculated as ^sK_a = ^sK_{MeOH}/^sK_{app}^{1/2}.

Kinetic Measurements. The rate of disappearance of **1** was followed by monitoring the decrease in absorbance of buffered methanol solutions at 240 nm with an OLIS modified Cary 17 UV-vis spectrophotometer or an Applied Photophysics SX-17MV stopped-flow reaction analyzer at 25.0 ± 0.1 °C. Reactions were monitored under pseudo-first-order conditions of excess metal ions in the range of (0.2–8.0) × 10⁻³ M and, in the case of slow reactions using conventional UV analysis, were initiated by addition of an aliquot of a 2.5 × 10⁻² M stock solution of **1** in CH₃CN to 2.5 mL of the buffered reaction mixture. The final concentration of amide was in the range (0.4–1.0) × 10⁻⁴ M. Reactions were followed for at least four half-lives and displayed good first-order behavior. Pseudo-first-order rate constants (*k*_{obs}) were determined by NLLSQ fitting of the absorbance vs time traces to a standard exponential model. *N*-Methylimidazole (^spK_a = 7.60), collidine (^spK_a = 7.72), *N*-methylmorpholine (^spK_a = 8.28), trimethylamine (^spK_a = 9.80^{6b}), triethylamine (^spK_a = 10.78^{6b}), and cyclohexylamine (^spK_a = 11.68^{6b}) buffers, partially neutralized with HClO₄, were used to control the ^spH. Total buffer concentrations varied between 10⁻³ and 10⁻² M. Oxalic acid (^spK_a = 5.54^{6b}) was used to control ^spH in the range 4–6 for methanolysis of **1** and **2**. All other measurements for these compounds between ^spH = 1 and 4, and above ^spH = 13, were done at constant [HClO₄] and [NaOCH₃]. ^spH measurements were performed before and after each experiment. To avoid any chloride ion contamination from the glass electrode which was found to affect the metal ion reactions, duplicate solutions were prepared: one for ^spH measurements, and the second for kinetics studies. In all cases, ^spH values measured before and after reaction were consistent to within 0.05 unit.

Due to the high sensitivity of [(NH₃)₅CoImCOCH₃](ClO₄)₃ to base-catalyzed methanolysis, special precautions were used. Stock solutions of [(NH₃)₅CoImCOCH₃](ClO₄)₃ were prepared in methanol containing 10⁻² M HClO₄, sonicated until all solid had dissolved, and then stored in an ice bath. For the La³⁺ reactions followed using the Applied Photophysics SX-17MV stopped-flow reaction analyzer, one drive syringe was charged with the slightly acidic (^spH = 4) methanol solution of [(NH₃)₅CoImCOCH₃](ClO₄)₃. The second drive syringe contained twice the desired concentration of La³⁺ salt and buffer. After mixing, the final substrate concentrations were between 1 × 10⁻⁴ and 5 × 10⁻⁴ M. Reactions were monitored at 240 nm, and the pseudo-first-order rate constants for methanolysis of **2** were determined in the same fashion as for **1**.

Results

a. Methanolysis of **1** and **2** in the Absence of Metal Ion.

Shown in Figure 1 are logarithmic plots of the observed rate constants (*k*_{obs}) vs ^spH for methanolysis of **1** and **2** in buffered methanol at 25 °C. The *k*_{obs} values were obtained at each ^spH using three to five buffer concentrations (in duplicate) between 10⁻³ and 10⁻² M and extrapolating to zero buffer concentration.

(10) Martell, A. E.; Motekaitis, R. *Determination and Use of Stability Constants*; VCH: New York, 1988.

(7) Jencks, W. P.; Carriuolo, J. *J. Biol. Chem.* **1959**, *234*, 1272. (b) Wolfenden, R.; Jencks, W. P. *J. Am. Chem. Soc.* **1961**, *83*, 4390. (c) Oakenfull, D. G.; Jencks, W. P. *J. Am. Chem. Soc.* **1971**, *93*, 178. (d) Oakenfull, D. G.; Jencks, W. P. *J. Am. Chem. Soc.* **1971**, *93*, 188. (e) Fife, T. H. *J. Am. Chem. Soc.* **1965**, *87*, 4597. (f) Palaitis, W.; Thornton, E. R. *J. Am. Chem. Soc.* **1975**, *97*, 1193. (g) Hogg, J. L.; Phillips, M. K.; Jergens, D. E. *J. Org. Chem.* **1977**, *42*, 2459. (h) Oakenful, P. G.; Jencks, W. P. *J. Am. Chem. Soc.* **1971**, *93*, 178. (i) Huskey, W. P.; Hogg, J. L. *J. Org. Chem.* **1981**, *46*, 53–59.

(8) Harrowfield, J. MacB.; Norris, V.; Sargeson A. M. *J. Am. Chem. Soc.* **1976**, *98*, 7282.

(9) Bates, R. *Determination of pH. Theory and Practice*; Wiley: New York, 1973.

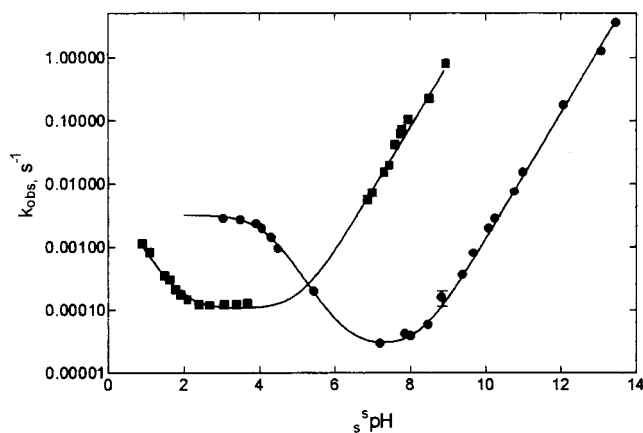
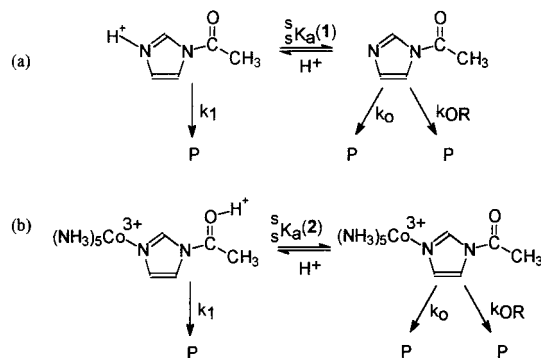


Figure 1. Logarithmic plot of observed rate constant of acetylimidazole **1** (●) and acetylimidazolepentaaminocobalt(III) perchlorate **2** (■) methanolysis vs s_{pH} at 25 °C. Curve calculated by nonlinear fit to eq 1 for **1** and eq 2 for **2**.

Scheme 1. Methanolysis of **1** (a) and **2** (b)



Methanolysis of **1** exhibited general-base-assisted buffer catalysis similar to that in water^{7h} (Brønsted β constant in MeOH = 0.89 ± 0.04), while that of **2** showed only minor buffer retardation, so extrapolation to [buffer] = 0 was not required for the latter. We note that, for these measurements, the ionic strength was not kept constant through the addition of salts but varied in proportion to the [buffer]. The extrapolated values for **1** thus are at $I = 0$, while those for **2** are at ionic strength $I < 0.02$. In addition, there is some small quantity of water present, the amount of $< 0.1\%$ stemming from that present in the supplied MeOH and that derived from buffer neutralization with 70% HClO₄. The presence of water at this low concentration does not influence the kinetics, *vide infra*.

The s_{pH} –rate constant plots for **1** and **2** can be accommodated by the mechanisms presented in Scheme 1, for which can be derived the rate expression given in eq 1, where k_1 and

$$k_{\text{obs}} = k_1 \left(\frac{[\text{H}^+]}{({}_sK_a^{(n)} + [\text{H}^+])} + (k_0 + k_{\text{OR}} \frac{{}_sK_{\text{MeOH}}}{[\text{H}^+]}) \frac{{}_sK_a^{(n)}}{({}_sK_a^{(n)} + [\text{H}^+])} \right) \quad (1)$$

k_0 represent the rate constants for attack of solvent on the protonated and neutral species, and k_{OR} that for attack of methoxide on **1** or **2**. In the case of **2**, since the kinetics are determined at $[\text{H}^+] \ll K_a$, the equation simplifies to the form given in eq 2, where $k_{\text{H}^+} = k_1 / {}_sK_a^{(2)}$.

$$k_{\text{obs}} = k_{\text{H}^+} [\text{H}^+] + k_0 + k_{\text{OR}} \frac{{}_sK_{\text{MeOH}}}{[\text{H}^+]} \quad (2)$$

NLLSQ fitting of the k_{obs} vs $[\text{H}^+]$ data for each amide to its respective equation generates the lines through the data in Figure

Table 1. Rate Constants for Solvolysis of Acetylimidazole (**1**) and [(NH₃)₅CoImCOCH₃](ClO₄)₃ (**2**) at 25 °C in Water and Methanol at Various Ionic Strengths

substrate	solvent	$10^5 k_0$ (s ⁻¹)	k_{H^+} (M ⁻¹ s ⁻¹)	k_{OR} (M ⁻¹ s ⁻¹)	$\frac{{}_wK_a}{\text{OR}}$ OR $\frac{{}_sK_a}{\text{pK}_a}$
1	H ₂ O ($I = 0.2$ M) ^a	8	1.87×10^2 ^e	320	3.6
	($I = 0.5$ M) ^b	5.6	3.2×10^2 ^e	290	
	($I = 1$ M) ^c	4.6			
	($I = 0$ M) ^d	30			
2	MeOH ($I = 0$ M)	2.6	5.2×10^2 ^e	7900	4.2
	H ₂ O ($I = 1$ M) ^c	110	5×10^{-4}	6860	
	MeOH ($I = 0$ M)	8.7	8.3×10^{-3}	4.69×10^7	

^a Reference 7a. ^b Reference 7f. ^c Reference 8. ^d Deiko, S.; Neverov, A.; Yatsimirskii, A. *Kinet. Catal.* **1989**, *30*, 694–698. ^e $k_{\text{H}^+} = k_1 / {}_sK_a$ or $k_1 / {}_wK_a$, depending on whether the solvent is methanol or water.

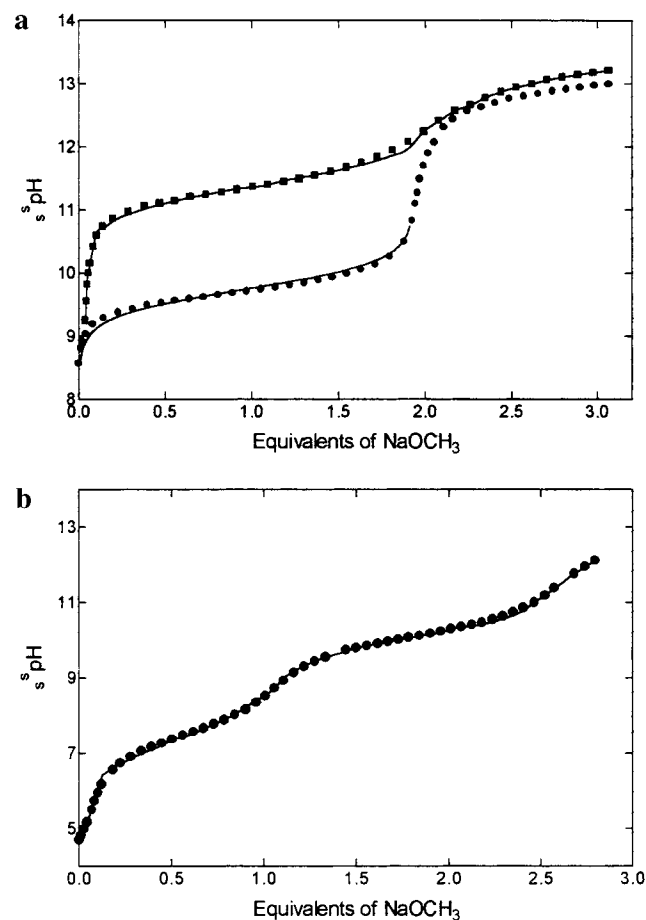
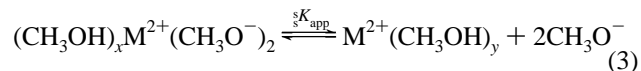


Figure 2. (a) pH titration of Zn(ClO₄)₂ (●) and Co(ClO₄)₂ (■) in methanol. (b) s_{pH} titration of 1.33×10^{-3} M La(OTf)₃ in methanol.

1, and the constants given in Table 1, the autoprotolysis constant⁶ for MeOH being set at $\text{p}K_{\text{MeOH}} = 10^{-16.77}$ M².

b. Metal Ion Titration. Potentiometric titration data for 1×10^{-4} M Zn(ClO₄)₂ and Co(ClO₄)₂ in methanol are shown in Figure 2a. Both metals show a steeper than standard titration curve with the consumption of 2 equiv of methoxide per metal. Equation 3 describes the process for double dissociation of the metal dimethoxide to form the probable hexakis(methanol)M²⁺ ions,¹¹ although the subscripts x and y refer to an unspecified



number of solvent molecules on the M²⁺. The $\text{p}K_a$'s calcu-

Table 2. Rate and Equilibrium Constants for Zn²⁺- and Co²⁺-Catalyzed Methanolysis of Acetylimidazole (**1**), *T* = 25 °C

metal	${}^sK_{\text{app}}^{\text{kinetic}} (\text{M}^2)$	${}^sK_{\text{app}}^{\text{titration}} (\text{M}^2)^a$	${}^sK_a^{\text{kinetic}} (\text{M})^b$ (${}^s\text{p}K_a$)	${}^sK_a^{\text{titration}} (\text{M})^c$ (${}^s\text{p}K_a$)	$k'_{\text{OR}} (\text{M}^{-2} \text{s}^{-1})^d$
Zn ²⁺	$10^{-14.21 \pm 0.04}$	$10^{-14.04}$	$10^{-9.67 \pm 0.04}$ (9.67)	$10^{-9.75}$ (9.75)	$(5.6 \pm 0.6) \times 10^8$
Co ²⁺	$10^{-11.89 \pm 0.08}$	$10^{-10.84}$	$10^{-10.82 \pm 0.08}$ (10.82)	$10^{-11.35}$ (11.35)	$(2.5 \pm 1.3) \times 10^8$

^a From titration fits to eq 3. ^b ${}^sK_a = {}^sK_{\text{MeOH}}/{}^sK_{\text{app}}^{1/2}$. ${}^sK_{\text{app}}^{\text{kinetic}}$ determined from fits of the kinetic data to eq 4; ${}^s\text{p}K_a$ refers to the pH at which 50% of the M^{2+} is in the inactive $\text{M}^{2+}(\text{CH}_3\text{O}^-)_2$ form. ^c ${}^sK_a = {}^sK_{\text{MeOH}}/{}^sK_{\text{app}}^{1/2}$. ${}^sK_{\text{app}}^{\text{titration}}$ determined from fits of titration data to eq 3. ^d $k'_{\text{OR}} = k_{\text{OR}}/K_{\text{M}}$, see text.

lated from the titration data (defined as the ${}^s\text{pH}$ at which 50% of the M^{2+} is in the inactive form, see Table 2) are 9.75 (Zn²⁺) and 11.35 (Co²⁺). In a separate set of experiments, the absorption spectrum for Co²⁺ was also monitored as a function of ${}^s\text{pH}$ to investigate possible ionization-dependent transformations from octahedral (pink) to tetrahedral coordination or pentacoordination (blue or violet). Progressing through the ${}^s\text{pH}$ range of 4.2–10.4, the Co²⁺ solutions ($(2.5\text{--}5.0) \times 10^{-3}$ M) turned yellow; no blue or violet was detected. At these concentrations, precipitates are formed at higher ${}^s\text{pH}$.

Given in Figure 2b is the potentiometric titration curve for La(OTf)₃ (1.33×10^{-3} M) in methanol, showing two ionization regions. The first, between ${}^s\text{pH}$ 6 and 9, results in consumption of 1 equiv of CH_3O^- per metal ion and can be treated as a normal ${}^s\text{p}K_a$, (${}^s\text{p}K_a = 7.22 \pm 0.15$). The second, around ${}^s\text{pH}$ 10, consumes 1.5 equiv of CH_3O^- per La³⁺, corresponding to a total of 2.5 equiv of H^+ per La³⁺ being released between ${}^s\text{pH}$ 6 and 12. This result can be explained by the formation of dimeric species at high ${}^s\text{pH}$ comprising two La³⁺ ions and five methoxide anions, analogous to what was proposed by Takasaki and Chin for a lanthanide dimer bridged by 5 OH^- in water.¹² Nonlinear fitting of the ${}^s\text{pH}$ /titrant data for the proposed dinuclear lanthanide complex with five ionizable protons using the PKAS program¹⁰ shows very good correlation with experimental data (Figure 2b).

c. Metal Ion Catalysis of Methanolysis. The water content present in the reaction mixture comes from three sources: (i) water present in the methanol (0.002%), (ii) the six hydrates present in the metal perchlorates, and (iii) the water present in 70% HClO_4 used to control ${}^s\text{pH}$. The first source is insignificant compared to the other two. In a solution containing 8×10^{-3} M buffer, the water present due to the acid varied from 0.005 to 0.02%, while the metal perchlorates contribute between 0.001 and 0.08%, depending on the concentration. Several kinetic experiments were performed using Zn(ClO₄)₂·6H₂O, Zn(ClO₄)₂·H₂O (produced by drying the Zn(ClO₄)₂·(H₂O)₆ under vacuum over P₂O₅ for 3 days), and Zn(CF₃SO₃)₂, and in all cases the k_{obs} values obtained were statistically equivalent. Furthermore, for the Co²⁺-catalyzed reactions at ${}^s\text{pH} = 9.74$, the trimethylamine buffer concentration was varied from 4×10^{-3} to 24×10^{-3} M with no effect on k_{obs} . Thus, the M^{2+} ion catalysis is insensitive to water concentrations up to 0.1% and also to buffer catalysis.

Both Zn²⁺ and Co²⁺ catalyze the methanolysis of **1**, and at each ${}^s\text{pH}$ the k_{obs} of methanolysis of **1** vs $[\text{M}^{2+}]$ gave a linear plot with no evidence of saturation up to a metal ion concentration of 8×10^{-3} M. With Co²⁺, precipitation occurred with concentrations as low as 2×10^{-3} M at ${}^s\text{pH} > 10.8$ but with lag times of 30 min to 12 h, depending on ${}^s\text{pH}$ and concentration. Kinetic runs above these ${}^s\text{pH}$'s were thus performed with

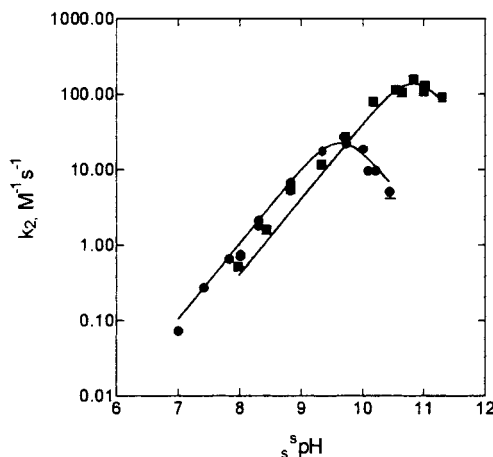
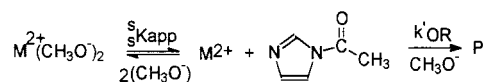


Figure 3. Logarithmic plot of second-order rate constants (k_2) of acetylimidazole methanolysis in the presence of Zn²⁺ (●) and Co²⁺ (■) against ${}^s\text{pH}$. Curve calculated by nonlinear fit of data to eq 4.

Scheme 2



much lower [Co²⁺] (10^{-5} – 10^{-4} M), with the aliquot of the stock Co²⁺ solution added just before measurements. Even so, for the Co²⁺-catalyzed reactions at high ${}^s\text{pH}$, we were forced to use stopped-flow kinetics because of the speed of the reaction. This in turn necessitates prolonged sample handling, with the possible consequence that some oligomerization of the Co²⁺-(OR⁻)_x occurs, causing a shift of the kinetic ${}^s\text{p}K_a$ toward lower ${}^s\text{pH}$ values, explaining the slight difference of the ${}^s\text{p}K_a$ kinetic and titrimetric values presented in Table 2.

We did not detect M^{2+} catalysis of the methanolysis of **2** (2×10^{-4} M) at ${}^s\text{pH} = 7.80$ (*N*-methylimidazole buffer, 4×10^{-3} M). In fact, both Zn²⁺ and Co²⁺ (up to 4×10^{-4} M) gave linear decelerations of the k_{obs} , probably due to an ionic strength effect.

Second-order rate constants (k_2) for metal ion catalysis of methanolysis of **1** were calculated from the slopes of the linear plots of k_{obs} vs $[\text{M}^{2+}]$ at each ${}^s\text{pH}$. The ${}^s\text{pH}$ vs k_2 profiles for Zn²⁺ and Co²⁺ shown in Figure 3 increase linearly with unit slope from ${}^s\text{pH} = 7\text{--}9.5$ and $8\text{--}10.5$, respectively, reaching maximum values and then dropping. Shown in Scheme 2 is a simplified mechanism that accounts for the ${}^s\text{pH}$ dependency, where P indicates the products imidazole and methyl acetate, with the metal dialkoxide being inactive, explaining the drop in rate at high ${}^s\text{pH}$. The expression given in eq 4 relates the second-order rate constants for metal ion catalysis of the attack of methoxide (k_2) to $[\text{H}^+]$, where ${}^sK_{\text{app}}$ is the apparent dis-

$$k_2 = k'_{\text{OR}} {}^sK_{\text{MeOH}} {}^sK_{\text{app}} \left(\frac{[\text{H}^+]}{([\text{H}^+]^2 {}^sK_{\text{app}} + {}^sK_{\text{MeOH}})} \right) \quad (4)$$

sociation constant for $\text{M}^{2+}(\text{CH}_3\text{O}^-)_2$ as in eq 3, k'_{OR} is a third-

(11) Sudbrake, C.; Müller, B.; Vahrenkamp, H. *Eur. J. Inorg. Chem.* **1999**, 2009.

(12) Takasaki, B. K.; Chin, J. *J. Am. Chem. Soc.* **1995**, *117*, 8582.

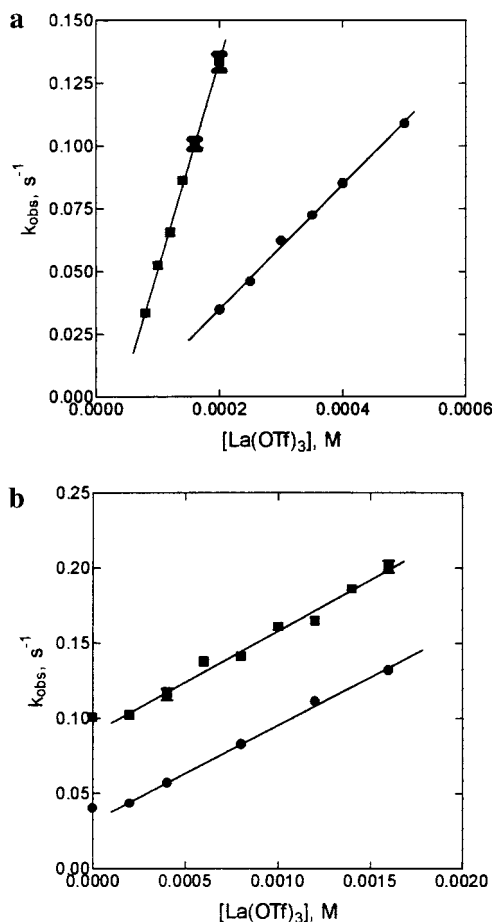


Figure 4. (a) Plot of pseudo-first-order rate constants for the methanolysis of AcIm vs $[\text{La}(\text{OTf})_3]$ at 25 °C; $\text{pH} = 9.1$ (■) and $\text{pH} = 7.33$ (●). (b) Plot of pseudo-first-order rate constants for the methanolysis of $\text{Co}(\text{NH}_3)_5\text{AcIm}$ vs $[\text{La}(\text{OTf})_3]$ at 25 °C; $\text{pH} = 7.95$ (■) and $\text{pH} = 7.6$ (●).

order rate constant for attack of methoxide on a $\text{M}^{2+}:\mathbf{1}$ complex ($k'_{\text{OR}} = k_{\text{OR}}/K_{\text{M}}$, where K_{M} is the dissociation constant for the putative $\text{M}^{2+}:\mathbf{1}$ complex) or a kinetic equivalent (vide infra), and ${}^sK_{\text{MeOH}}$ is the autoprotolysis constant of methanol. NLLSQ fitting of the k_2 vs $[\text{H}^+]$ data to eq 4 generates the constants given in Table 2 and the lines through the data in Figure 2.

Pseudo-first-order rate constants, k_{obs} , as a function of $[\text{La}^{3+}]$ obtained for the methanolysis of **1** and **2** at a given pH show strong catalysis by $\text{La}(\text{OTf})_3$, with the effect being pH -sensitive and linearly proportional to $[\text{La}(\text{OTf})_3]$ at higher concentrations of metal salt (see Figure 4) but with significant curvature at concentrations lower than $\sim 2 \times 10^{-4}$ M (see Figure 5). This indicates the involvement of second-order terms in $[\text{La}(\text{OTf})_3]$. Unfortunately, direct kinetic analysis of all the experimental k_{obs} vs $[\text{La}^{3+}]_t$ data does not provide reliable parameters, particularly in the case of **2** due to the high rate of the background reaction. However, the fact that the k_{obs} vs $[\text{La}(\text{OTf})_3]_t$ dependencies look very similar for both substrates eliminates any possibility that the higher reaction order in $[\text{La}^{3+}]$ is due to complexation of a La^{3+} ion by the distal nitrogen of **1**, and rather indicates a concentration-dependent change in speciation of $\text{La}(\text{OTf})_3$ in methanol solution such as formation of soluble dimers. Analysis of the linear parts of the plots (Figure 4) gives the second-order rate constants (k_2), which are then plotted versus pH as in Figure 6, revealing similar profiles for both **1** and **2** with apparent kinetic pK_a 's of 7–7.5.

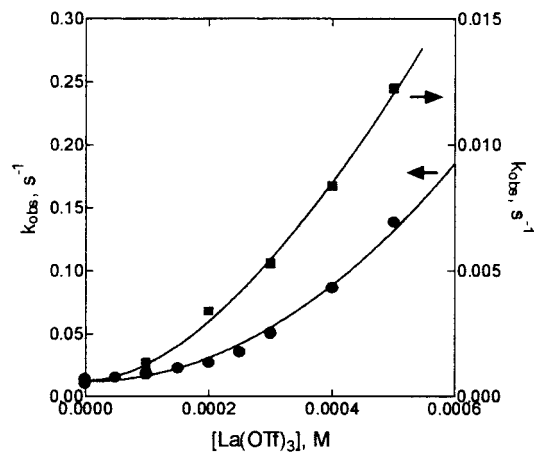


Figure 5. Plots of pseudo-first-order rate constants vs $[\text{La}^{3+}]$ for the methanolysis of AcIm (■, right axis, $\text{pH} = 6.7$) and $\text{AcImCo}(\text{NH}_3)_5^{3+}$ (●, left axis, $\text{pH} = 7.6$, $I = 0.2$ (NaClO_4)) at 25 °C.

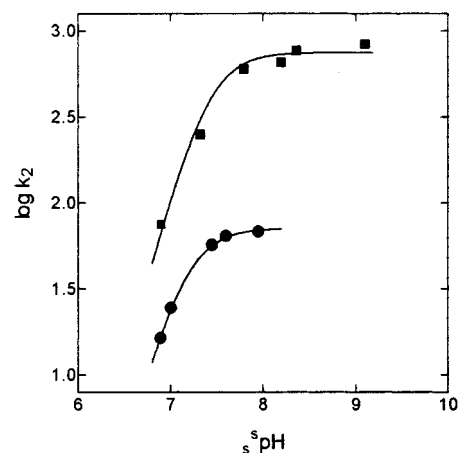
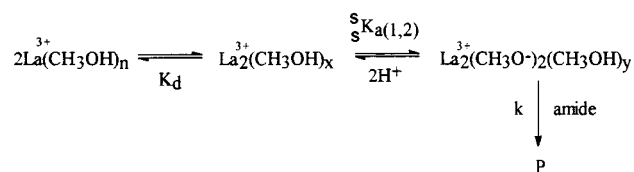


Figure 6. Plots of second-order rate constant (k_2) vs pH for $\text{La}(\text{OTf})_3$ -catalyzed methanolysis of AcIm (■) and $\text{AcImCo}(\text{NH}_3)_5^{3+}$ (●). Curves are the result of NLLSQ fitting of experimental data to eq 7.

Scheme 3



As described above, potentiometric titration of $\text{La}(\text{OTf})_3$ (1.33 mmol) in methanol shows ionization of one proton per metal ion in the pH region of interest (6–9), with $\text{pK}_a = 7.22 \pm 0.15$ (see Figure 2b). In combination with the pH -rate profiles (Figure 6) and the k_{obs} vs $[\text{La}(\text{OTf})_3]$ dependencies (Figure 5), this indicates that the kinetically active species is a dimeric complex consisting of two La^{3+} ions and two methoxide anions with an unspecified number of solvent molecules as shown in Scheme 3, where ${}^sK_{\text{a}(1,2)}$ refers to the product of the first and second H^+ dissociation constants of the dimer. The equations for the equilibrium constants and the conservation of mass pertaining to the process in Scheme 3 provide the expression for the rate constant given in eq 5. The linear part

$$k_{\text{obs}} = k_0 + (k {}^sK_{\text{a}(1,2)}[\text{H}^+]^2/K_d) \left((1 + 8({}^sK_{\text{a}(1,2)} + [\text{H}^+]^2)K_d[\text{La}^{3+}]_t/[\text{H}^+]^2)^{-1} / (4({}^sK_{\text{a}(1,2)} + [\text{H}^+]^2))^2 \right) \quad (5)$$

of the plots of k_{obs} vs $[\text{La}^{3+}]_t$ (Figure 5) used to calculate the

second-order rate constant k_2 describe the conditions where $\delta k_{\text{obs}}/\delta[\text{La}^{3+}]_t$ is constant (eq 6), where $\alpha = {}^sK_{\text{a}(1,2)}[\text{H}^+]^2/$

$$k_2 = \delta k_{\text{obs}}/\delta[\text{La}]_t = k\alpha\beta(1 - 1/(1 + \beta[\text{La}^{3+}]_t)^{0.5}) \quad (6)$$

$(16K_{\text{d}}({}^sK_{\text{a}(1,2)} + [\text{H}^+]^2)^2)$, and $\beta = 8K_{\text{d}}({}^sK_{\text{a}(1,2)} + [\text{H}^+]^2)/[\text{H}^+]^2$. To satisfy the condition that $\delta k_{\text{obs}}/\delta[\text{La}^{3+}]_t$ is constant, the range of $[\text{La}^{3+}]_t$ for analysis must be chosen such that $(1 + \beta[\text{La}^{3+}]_t)^{0.5}$ must be much bigger than 1, thereby providing an expression relating k_2 to ${}^sK_{\text{a}(1,2)}$ (eq 7). NLLSQ fitting of ${}^s\text{pH}-k_2$ data

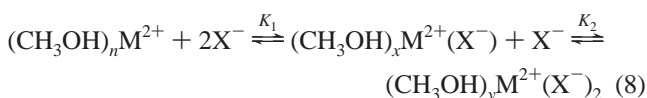
$$k_2 = k {}^sK_{\text{a}(1,2)} / (2({}^sK_{\text{a}(1,2)} + [\text{H}^+]^2)) \quad (7)$$

(Figure 6) to eq 7 gives the following parameters: $k = (1.50 \pm 0.1) \times 10^3 \text{ M}^{-1} \text{ s}^{-1}$, $K_{\text{a}(1,2)} = 10^{(-14.8 \pm 0.1)} \text{ M}^2$ (kinetic ${}^s\text{p}K_{\text{a}} = 7.40$) for **1**; and $k = (1.42 \pm 0.02) \times 10^2 \text{ M}^{-1} \text{ s}^{-1}$, ${}^sK_{\text{a}(1,2)} = 10^{(-14.30 \pm 0.02)} \text{ M}^2$ (kinetic ${}^s\text{p}K_{\text{a}} = 7.15$) for **2**. The lines through the data in Figure 6 are those generated by the fits using these values.

Discussion

a. Methanolysis of 1 and 2. The pH-rate profiles for methanolysis of **1** and **2** (Figure 1) bear a striking resemblance to those determined in water,^{7,8} suggesting similar mechanisms having acid, neutral, and base domains for both reactions. The kinetic ${}^s\text{p}K_{\text{a}}$ of 4.2 determined for **1**-H⁺ in methanol is slightly above its water ${}^w\text{p}K_{\text{a}}$ (3.6),⁷ generally agreeing with the relative trends in ${}^s\text{p}K_{\text{a}}$ for nitrogen-protonated bases in methanol^{6b} that show slight increases (0.2–0.4) compared to their ${}^w\text{p}K_{\text{a}}$'s in water. The most notable differences between the water and methanol kinetic parameters for solvolysis of **1** given in Table 1 concern the attack of HOR (k_0) and ⁻OR (k_{OR}), where methanol is about 10 times poorer a nucleophile than water (at $I = 0$), but methoxide in methanol is 26 times more reactive than hydroxide in water. Comparison of the data for the ligand-exchange-inert and positively charged Co^{3+} complex **2** provides evidence for a much stronger solvent effect on the attack of lyoxide. In water, attack of hydroxide on **2** increases only 24-fold relative to ⁻OH attack on **1**, but attack of CH_3O^- in methanol is accelerated 5900-fold. The accelerated attack of anions on cationic **2** in MeOH relative to that in H_2O is anticipated on electrostatic grounds since the attractive forces between oppositely charged ions is inversely proportional to the dielectric constant of the medium.¹³

b. Potentiometric Titration of Zn^{2+} , Co^{2+} , and La^{3+} in Methanol. Potentiometric titration of both Zn^{2+} and Co^{2+} consumes 2 equiv of CH_3O^- per metal by ${}^s\text{pH} \sim 10$ and ~ 12 . The steep profile for consumption of CH_3O^- shown in Figure 2a cannot be accommodated by the stepwise process given in eq 8, $\text{X} = \text{CH}_3\text{O}^-$, unless there is cooperativity in association of the second methoxide such that $K_2 > K_1$. While this



phenomenon has not yet been described for metal alkoxides, it is of note that zinc halides ($\text{X} = \text{Cl}$, Br and I) show a preference

for the formation of the bis-halide compared to the mono-halide in DMSO¹⁴ and methanol.¹⁵ Doe and Kitagawa^{15a} determined K_1 and K_2 stability constants for $\text{Zn}-\text{Cl}$ in methanol of $(7.76 \pm 0.18) \times 10^3$ and $(1.74 \pm 0.10) \times 10^4 \text{ M}^{-1}$. This unusual effect was attributed to a change in the Zn^{2+} complex structure accompanying the binding of Cl^- , leading to a difference in charge density between the central metal as it transforms from an octahedral structure ($\text{Zn}^{2+}(\text{MeOH})_6$) to a tetrahedral one, $\text{ZnX}_2(\text{MeOH})_2$, and the entropy effect from the decrease in the number of coordinating MeOH molecules substituted by Cl^- . A similar sort of explanation likely accounts for the preferential formation of Zn^{2+} and Co^{2+} dimethoxides. Clearly, association of CH_3O^- with the metal would liberate several of its solvating methanols also, contributing to the entropy effect. In the case of $\text{Co}^{2+}(\text{CH}_3\text{O}^-)_2$, we have checked for the appearance of tetrahedral or five-coordinate Co^{2+} by UV/vis spectroscopy, but we have found no evidence for blue colors, suggesting that the coordination must still be octahedral.

The titration shown in Figure 2b for La^{3+} indicates that there is a stepwise association of one CH_3O^- per La^{3+} (${}^s\text{p}K_{\text{a}} = 7.22$) and a second event occurring between ${}^s\text{pH}$ 10 and 11, consuming $1.5\text{CH}_3\text{O}^-/\text{La}^{3+}$. These data, taken together with the curved k_{obs} vs $[\text{La}^{3+}]$ plots for methanolysis given in Figure 5, suggest that a dimeric species is formed which we show later is kinetically active between ${}^s\text{pH}$ 6 and 9. Dimeric structures are not unknown for lanthanum ions and were previously observed in methanol solutions of LaCl_3 by using La^{139} and Cl^{35} NMR.¹⁶

c. Metal Ion Catalysis of Methanolysis. (i) Zn^{2+} and Co^{2+} . Zn^{2+} and Co^{2+} catalyze methoxide addition to **1** by a process that is first order in each of $[\text{M}^{2+}]$ and $[\text{CH}_3\text{O}^-]$. The proposed mechanism involves formation of inactive $\text{M}^{2+}(\text{CH}_3\text{O}^-)_2$ at high $[\text{CH}_3\text{O}^-]$, explaining the drop in catalysis seen in Figure 3 above ${}^s\text{pH}$ 10 and 11 for Zn^{2+} and Co^{2+} , respectively. The values provided in Table 2 from the fits of the k_2 data for metal ion catalysis vs $[\text{H}^+]$ to eq 4 indicate a large third-order rate constant (k'_{OR}) for the reaction of $(\text{CH}_3\text{O}^- + \text{M}^{2+} + \mathbf{1})$ or various kinetic equivalents such as CH_3O^- attack on a transient $\text{M}^{2+}:\mathbf{1}$ complex, or reaction of $\text{M}^{2+}:\text{CH}_3\text{O}^- + \mathbf{1}$. In what follows we will provide evidence limiting these possibilities.

In aqueous solution, there are generally two mechanisms that are proposed for metal-ion-promoted reaction of OH^- on $\text{C}=\text{O}$ units: the metal-bound hydroxide ($\text{M}^{2+}-\text{OH}^-$) mechanism and the metal plus external hydroxide ($\text{M}^{2+} + \text{OH}^-$) mechanism.¹ It is often difficult to distinguish these kinetically equivalent possibilities, but one way is to rule out a mechanism because the rate constant for the reaction would exceed diffusion control. This approach was used by Fife and Przystas¹⁷ to show that the Cu^{2+} -catalyzed hydrolysis of *N*-(6-carboxypicolinyl)-benzimidazole must proceed through a complexed $\text{Cu}^{2+}-\text{OH}^-$.

Involvement of metal alkoxide as an active species in the M^{2+} -promoted methanolysis of **1** can be ruled out by a combination of titration data indicating sharp consumption of 2 equiv of CH_3O^- by M^{2+} (Figure 2a) and by the unit slope of the log plots of the second-order rate constant for metal ion catalysis vs ${}^s\text{pH}$ shown in Figure 3. Were the $\text{M}^{2+}-\text{OCH}_3^-$ the active form, it would necessarily be depleted through equilibrium

(14) Ahrlund, S.; Björk, N.-O. *Acta Chem. Scand. A* **1976**, *30*, 265. (b) Ahrlund, S.; Björk, N.-O.; Portanova, R. *Acta Chem. Scand. A* **1976**, *30*, 270.

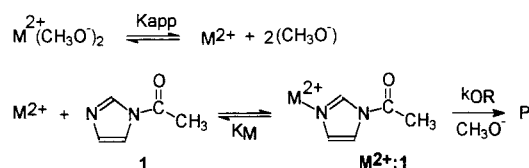
(15) Doe, H.; Kitagawa, T. *Inorg. Chem.* **1982**, *21*, 2272. (b) Doe, H.; Shibagaki, A.; Kitagawa, T. *Inorg. Chem.* **1983**, *22*, 1639.

(16) Smith, L. S.; McCain, D. C.; Wertz, D. L. *J. Am. Chem. Soc.* **1976**, *98*, 5125.

(17) Fife, T. H.; Przystas, T. J. *J. Am. Chem. Soc.* **1986**, *108*, 4631.

(13) Harned, H. S.; Owen, B. B. *The Physical Chemistry of Electrolytic Solutions*, 3rd ed.; ACS Monograph Series 137; Reinhold Publishing: New York, 1957; pp 42–58.

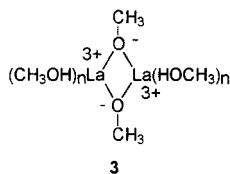
Scheme 4



formation of inactive $\text{M}^{2+}(\text{CH}_3\text{O}^-)_2$ at increasing pH, such that the log plots of the rate constant for metal ion catalysis vs pH would not have a unit slope but would be curved downward.

Thus, the most reasonable mechanism involves attack of external methoxide on a transiently formed $\text{M}^{2+}:1$ complex as in Scheme 4, which is a slightly expanded version of Scheme 2. Notably, the plots of k_{obs} vs $[\text{M}^{2+}]$ are strictly linear up to at least 8×10^{-3} M and show no evidence of saturation binding, suggesting a lower limit for the K_{M} value of ~ 0.1 M. We attempted to determine a better value for the binding constant by performing a competition experiment¹⁸ between H^+ and Zn^{2+} for acetylimidazole at $\text{pH} = 3.94$. At this value there is no appreciable methoxide reaction, but the acid-promoted reaction might be perturbed to lower pH values due to equilibrium binding of the metal ion. At a $[\text{Zn}^{2+}]$ of 2×10^{-2} M, no change in the rate constant for acid-catalyzed methanolysis is observed, again supporting a lower limit of ~ 0.1 M for K_{M} . Combining this value with the $k'_{\text{OR}} = k_{\text{OR}}/K_{\text{M}}$ terms given in Table 2 gives rate constants for methoxide attack on $1:\text{M}^{2+}$ (k_{OR}) of 5.6×10^7 and 2.5×10^7 $\text{M}^{-1} \text{s}^{-1}$ for Zn^{2+} and Co^{2+} , respectively. These values compare favorably with the rate constant for attack of CH_3O^- on the Co^{III} complex **2**, given in Table 1 as 4.69×10^7 $\text{M}^{-1} \text{s}^{-1}$. Of course, it is difficult to assess the relative modes of activation of methoxide attack by coordinated $(\text{NH}_3)_5\text{Co}^{3+}$ and $(\text{CH}_3\text{OH})_x\text{M}^{2+}$, but the results clearly indicate that coordination leads to a reaction which is only 100 times less than the diffusion limit.¹⁹ The most reasonable site of complexation, based on relative basicities, is the distal N and not the C=O unit.

(ii) La^{3+} . As shown in Figure 5, plots of the methanolysis of both **1** and **2** vs $[\text{La}^{3+}]$ are curved upward, suggesting a process that is bimolecular in metal ion. This observation, coupled with the titration data indicating the consumption of one CH_3O^- per La^{3+} ($\text{p}K_{\text{a}} = 7.22$), indicates that the catalytically active form is a La dimer with two associated methoxides, formulated simply as **3** with an unspecified number of coordinated molecules. At



increased $[\text{La}^{3+}]$, the kinetic plots shown in Figure 4 for both **1** and **2** become linear, the slope at each pH being the second-order rate constant, k_2 , for dimer-promoted methanolysis. Plots of these vs pH (Figure 6) show a sharp rise (slope ~ 2 , as required for the involvement of two methoxides), followed by

(18) Neverov, A. A. Ph.D. Dissertation, Moscow State University, 1991. Neverov uses the competition between metal ion and H^+ to displace the normal acid-catalyzed reaction of acetyl imidazole to lower pH values. He reports that for the reaction of acetyl imidazole in water with Zn^{2+} and Ni^{2+} , the respective K_{M} values for the dissociation $\text{AcIm}:\text{M}^{2+} \rightleftharpoons \text{AcIm} + \text{M}^{2+}$ are 3.5×10^{-2} M ($[\text{Zn}^{2+}] = 0.1$ M, ZnCl_2) and 7.3×10^{-3} M ($[\text{Ni}^{2+}] = 0.2$ M, NiCl_2).

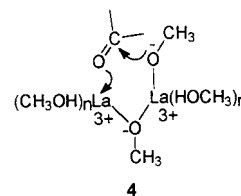
(19) Engen, M.; De Maeyer, L. Z. *Electrochem.* **1955**, *59*, 986.

a plateau, with apparent kinetic $\text{p}K_{\text{a}}$'s of 7.40 and 7.15 for **1** and **2** determined by fitting the data to eq 7. These kinetic values are in close agreement with what is determined for the apparent $\text{p}K_{\text{a}}$ by potentiometric titration, lending strong credence to the validity of the suggested model. The fits also provide maximal second-order rate constants of 1.5×10^3 and 1.42×10^2 $\text{M}^{-1} \text{s}^{-1}$ for methanolysis of **1** and **2** catalyzed by the dimer.

Similar double-bridge structures were suggested for $\text{La}_2\text{Cl}_6(\text{CH}_3\text{OH})_{10}$ ²⁰ (with bridging chloride ions) and a La^{3+} -peroxide complex (with bridging peroxide dianions).¹² From a study of the hydrolysis of an RNA model dimer promoted by La^{3+} in water, Hurst, Takasaki, and Chin²¹ proposed a similar catalytically active structure having two lanthanide ions bridged by five HO^- .

Comparison of the second-order rate constants (k) for La^{3+} -promoted methanolysis of **1** and **2** clearly indicates that coordination of the $(\text{NH}_3)_5\text{Co}^{3+}$ to the distal nitrogen does not provide any enhancement of the catalytic effect of La^{3+} . Even though **2** has a much better leaving group than does **1** ($\text{p}K_{\text{a}} = 10.0$ for $-\text{ImCo}(\text{NH}_3)_5^{3+}$ vs 14 for Im^{2-}), the rate of its La^{3+} -promoted reaction is 10-fold slower. This contrasts our results for CH_3O^- -catalyzed methanolysis of **2** given in Table 1, where the second-order rate constant $k_{\text{OR}} = 4.69 \times 10^7$ $\text{M}^{-1} \text{s}^{-1}$ is 5900-fold higher than that for CH_3O^- on **1** ($k_{\text{OR}} = 7.9 \times 10^3$ $\text{M}^{-1} \text{s}^{-1}$). Strong acceleration of methoxide attack on **2** relative to that on **1** can be explained by a combination of leaving group effects and electrostatic interaction between the positively charged substrate (**2**) and a negatively charged nucleophile. The fact that the La^{3+} -promoted methanolysis reaction is slower with **2** probably obviates attack of free methoxide ion, since that should result in much higher rate constants for **2** than for **1**, contrary to what is observed. The slower reaction of the lanthanide reaction with **2** is best accommodated by a mechanism where the reactive species is the dimeric complex $(\text{La}^{3+}_2(\text{CH}_3\text{O}^-)_2(\text{CH}_3\text{OH})_y)$ (**3**), having a total positive charge of 4+, wherein electrostatic repulsion causes a decrease in the rate for the positively charged substrate **2** relative to neutral **1**.

It has been shown in the case of a structurally similar Co^{3+} -hydroxide dimeric complex that bridging hydroxides are not nucleophilic, being at least 10^{10} times less active than their deprotonated oxo-bridged forms.²³ The same should be true for a bridging CH_3O^- , but clearly the proposed methoxy-bridged La^{3+} dimer (**3**) cannot be further deprotonated, so the only way to generate an active nucleophile within the dimeric complex requires temporary breakage of a La^{3+} -methoxy bond. This creates a nucleophilic/electrophilic center where the La^{3+} -bound methoxy can attack the C=O carbon, with the second La^{3+} functioning as a Lewis acid to stabilize the developing negative charge on carbonyl oxygen as in **4**.



(20) Smith, L. S.; McCain, D. C.; Wertz, D. L. *J. Am. Chem. Soc.* **1976**, *98*, 5125.

(21) Hurst, P.; Takasaki, B. K.; Chin, J. *J. Am. Chem. Soc.* **1996**, *118*, 9982.

(22) Sundberg, R. J.; Martin, R. B. *Chem. Rev.* **1974**, *74*, 471.

(23) Wahnon, D.; Lebus, A.-M.; Chin, J. *Angew. Chem., Int. Ed. Engl.* **1995**, *34*, 2412. (b) Williams, N. H.; Lebus, A.-M.; Chin, J. *J. Am. Chem. Soc.* **1999**, *121*, 3341.

Conclusions

Recent seminal investigations by Bosch and co-workers⁶ have shown that $s_p\text{H}$ measurement and control with buffers in methanol solution can be done as simply as in water. This opens up the possibility for detailed kinetic studies of various acyl and phosphoryl transfer reactions in methanol which can then be readily compared with hydrolyses. In the above we have shown the following:

1. Metal ions such as Zn^{2+} and La^{3+} are soluble in methanol throughout the entire pH range of interest without the formation of insoluble $\text{M}^{x+}(\text{OR}^-)_n$ precipitates during the kinetics which so often accompany deprotonation of metal-aquo complexes in water. Co^{2+} is less soluble at high pH values, but the $\text{Co}^{2+}(\text{CH}_3\text{O}^-)_2$ species is sufficiently soluble for a limited time that allows one to determine the kinetic effect on methanolysis of **1**.

2. Unlike hydrolysis, methanolysis of the activated amide acetylimidazole (**1**) is subject to marked metal ion catalysis by Zn^{2+} and Co^{2+} . In the case of the divalent metal ions the catalysis does not involve $\text{M}^{2+}(\text{CH}_3\text{O}^-)_n$ forms, but rather involves attack of external methoxide on a metal:**1** complex. The rate constants for methoxide attack on $\text{Zn}^{2+}:\mathbf{1}$, $\text{Co}^{2+}:\mathbf{1}$, and $(\text{NH}_3)_5\text{Co}^{3+}:\mathbf{1}$ are 5.6×10^7 , 2.5×10^7 , and $4.69 \times 10^7 \text{ M}^{-1} \text{ s}^{-1}$ respectively, roughly 10^4 -fold greater than CH_3O^- attack on **1** itself ($7.9 \times 10^3 \text{ M}^{-1} \text{ s}^{-1}$). It is tempting to suggest that the reason that the divalent metal ions so strongly promote methanolysis but not hydrolysis is that attack of anions on the positively charged $\text{M}^{2+}:\mathbf{1}$ transient is promoted by the increase in electrostatic interaction in methanol relative to that in water. The fact that these metal ions do promote the methanolysis of **1** but not **2** suggests that the site of complexation is the distal N and not the C=O group.

3. La^{3+} exists in methanol solution above $s_p\text{H}$ 7.5 as a $(\text{La}^{3+}(\text{CH}_3\text{O}^-))_2$ -bridged dimer that promotes methanolysis of both **1** and **2** with second-order rate constants of 1.5×10^3 and $1.42 \times 10^2 \text{ M}^{-1} \text{ s}^{-1}$. The mechanism by which the methanolysis occurs cannot involve coordination to the distal N with attack of external CH_3O^- , as in the case of Zn^{2+} , Co^{2+} , or $(\text{NH}_3)_5\text{Co}^{3+}$, but rather involves direct attack on the C=O group, probably by temporarily releasing a bridging methoxide from

one La^{3+} to reveal an open form of the dimer where one La^{3+} acts as a Lewis acid to activate attack of the second La^{3+} -bound methoxide.

In the past decade, much attention was focused on the remarkable acceleration provided by lanthanide cations (Ln^{x+}) for the hydrolysis of phosphate esters^{12,24} and, to a lesser degree, amides and peptides.²⁵ However, mechanistic study of these Ln^{x+} -promoted hydrolyses is hindered by the fact that, in water, formation of insoluble hydroxides and gels of poor definition is a problem, particularly under basic conditions.²⁶ The results presented above indicate that metal ion reactions can now be studied in methanol without the formation of precipitates during the kinetic analysis. Furthermore, in the case of La^{3+} -promoted methanolyses, a soluble and kinetically active bis-methoxy-bridged La dimer is present in solution. It appears that the methanol medium stabilizes formation of this dimer without the necessity of coordinating it to stabilizing ligands. Given that the site of reaction seems to be the C=O group of the substrate, work is currently underway in our laboratories to see whether these, and related, La^{3+} dimers will promote the methanolyses of more biologically relevant species such as nonactivated esters, amides, and phosphates.

Acknowledgment. The authors gratefully acknowledge the financial support of the Natural Sciences and Engineering Research Council of Canada. We also acknowledge the helpful suggestions of a reviewer.

JA0023940

(24) Blasko, A.; Bruice, T. C. *Acc. Chem. Res.* **1999**, *32*, 475 and references therein. (b) Williams, N. H.; Tasaki, B.; Wall, M.; Chin, J. *Acc. Chem. Res.* **1999**, *32*, 485 and references therein. (c) Moss, R. A.; Park, B. D.; Scrimin, P.; Ghirlanda, G. *J. Chem. Soc., Chem. Commun.* **1995**, 1627. (d) Moss, R. A.; Zhang, J.; Bracken, K. *J. Chem. Soc., Chem. Commun.* **1997**, 1639. (e) Sumaoka, J.; Miyama, S.; Komiyama, M. *J. Chem. Soc., Chem. Commun.* **1994**, 1755. (f) Morrow, J. R.; Buttrey, L. A.; Berback, K. A. *Inorg. Chem.* **1992**, *31*, 16. (g) Morrow, J. R.; Buttrey, L. A.; Shelton, V. M.; Berback, K. A. *J. Am. Chem. Soc.* **1992**, *114*, 1903. (h) Breslow, R.; Zhang, B. *J. Am. Chem. Soc.* **1994**, *116*, 7893. (i) Takeda, N.; Irisawa, M.; Komiyama, M. *J. Chem. Soc., Chem. Commun.* **1994**, 2773.

(25) Takarada, T.; Takahashi, R.; Yashiro, M.; Komiyama, M. *J. Phys. Org. Chem.* **1998**, *11*, 41. (b) Yashiro, M.; Takarada, T.; Miyama, S.; Komiyama, M. *J. Chem. Soc., Chem. Commun.* **1994**, 1757.

(26) Gómez-Tagle, P.; Yatsimirsky, A. K. *J. Chem. Soc., Dalton Trans.* **1998**, 2957.